

# Alu antisense RNA ameliorates methylglyoxal-induced human lens epithelial cell apoptosis by enhancing antioxidant defense

Pei-Yuan Wu<sup>1</sup>, Ning Ji<sup>1</sup>, Chong-Guang Wu<sup>1</sup>, Xiao-Die Wang<sup>1</sup>, Xin Liu<sup>1</sup>, Zhi-Xue Song<sup>1</sup>, Murad Khan<sup>1</sup>, Suleman Shah<sup>1</sup>, Ying-Hua Du<sup>2</sup>, Xiu-Fang Wang<sup>1</sup>, Li-Fang Yan<sup>1</sup>

<sup>1</sup>Department of Genetics, Hebei Medical University, Hebei Key Lab of Laboratory Animal, Shijiazhuang 050017, Hebei Province, China

<sup>2</sup>Department of Ophthalmology, Beijing Tiantan Hospital, Capital Medical University, Beijing 100070, China

**Co-first authors:** Pei-Yuan Wu and Ning Ji

**Correspondence to:** Xiu-Fang Wang and Li-Fang Yan. Department of Genetics, Hebei Medical University, Hebei Key Lab of Laboratory Animal, 361 Zhongshan East Road, Shijiazhuang 050017, Hebei Province, China. wangxf1966@hebmu.edu.cn; lifangyiyaa@163.com

Received: 2022-06-22 Accepted: 2022-11-29

## Abstract

• **AIM:** To determine whether an antisense RNA corresponding to the human Alu transposable element (Aluas RNA) can protect human lens epithelial cells (HLECs) from methylglyoxal-induced apoptosis.

• **METHODS:** Cell counting kit-8 (CCK-8) and 3-(4,5-Dimethylthiazol-2-yl)-2,5-diphenyltetrazolium bromide (MTT) assays were used to assess HLEC viability. HLEC viability/death was detected using a Calcein-AM/PI double staining kit; the annexin V-FITC method was used to detect HLEC apoptosis. The cytosolic reactive oxygen species (ROS) levels in HLECs were determined using a reactive species assay kit. The levels of malondialdehyde (MDA) and the antioxidant activities of total-superoxide dismutase (T-SOD) and glutathione peroxidase (GSH-Px) were assessed in HLECs using their respective kits. RT-qPCR and Western blotting were used to measure mRNA and protein expression levels of the genes.

• **RESULTS:** Aluas RNA rescued methylglyoxal-induced apoptosis in HLECs and ameliorated both the methylglyoxal-induced decrease in Bcl-2 mRNA and the methylglyoxal-induced increase in Bax mRNA. In addition, Aluas RNA inhibited the methylglyoxal-induced increase in Alu sense RNA expression. Aluas RNA inhibited the production of ROS induced by methylglyoxal, restored T-SOD and GSH-

Px activity, and moderated the increase in MDA content after treatment with methylglyoxal. Aluas RNA significantly restored the methylglyoxal-induced down-regulation of Nrf2 gene and antioxidant defense genes, including glutathione peroxidase, heme oxygenase 1,  $\gamma$ -glutamylcysteine synthetase and quinone oxidoreductase 1. Aluas RNA ameliorated methylglyoxal-induced increases of the mRNA and protein expression of Keap1 that is the negative regulator of Nrf2.

• **CONCLUSION:** Aluas RNA reduces apoptosis induced by methylglyoxal by enhancing antioxidant defense.

• **KEYWORDS:** human Alu antisense RNA; human lens epithelial cells; methylglyoxal toxicity; antioxidant defense; apoptosis

**DOI:10.18240/ijo.2023.02.03**

**Citation:** Wu PY, Ji N, Wu CG, Wang XD, Liu X, Song ZX, Khan M, Shah S, Du YH, Wang XF, Yan LF. Alu antisense RNA ameliorates methylglyoxal-induced human lens epithelial cell apoptosis by enhancing antioxidant defense. *Int J Ophthalmol* 2023;16(2):178-190

## INTRODUCTION

Growing evidence indicates that cataractogenic stresses can result in the production of misfolded proteins by the endoplasmic reticulum (ER)<sup>[1]</sup>. To reduce misfolded proteins from cells before the stresses induce senescence, the cells produce a cascade of reactions called ER stress<sup>[2-3]</sup>. ER stress upregulates the production of intracellular reactive oxygen species (ROS) and activates Nrf2, a central transcriptional factor for protecting cell against stress, in order to maintain cellular redox homeostasis by regulating the expression of a group of genes that protect cells<sup>[4-5]</sup>. Nrf2 is normally localized to the cytosol *via* binding with its negative regulator Keap1, which is in turn bound to cytosolic actin<sup>[1]</sup>. Nrf2 binds with Keap 1 under non-stress conditions; upon oxidative/ER stress, Nrf2 isolates from Keap1, translocates to the nucleus, and activates the expression of a number of antioxidant-related genes<sup>[6-8]</sup>. The Nrf2 pathway is believed to regulate as many as 600 cytoprotective genes<sup>[9-12]</sup>.

Methylglyoxal (MGO) is a reactive carbonyl aldehyde compound that is an end product of glycolysis. MGO is cytotoxic and induces cell apoptosis by inducing the production of ROS<sup>[13]</sup>. These negative effects underlie the role of MGO as a mediator of the secondary complications of diabetes mellitus, including cataracts<sup>[14-15]</sup>. In the eye, the ROS causes cellular damage that induces cataract formation<sup>[16]</sup>.

Short interspersed nuclear elements (SINEs) occupy approximately 10% of the mammalian genome<sup>[17-18]</sup>. Alu elements are the main SINEs in the human genome<sup>[17-19]</sup>. These Alu elements can be transcribed into Alu RNA. The expression of Alu RNA increases under oxidative stress and after infection by viruses<sup>[20-21]</sup>. Alu RNA levels may also be associated with the development of disease; for example, the accumulation of Alu RNA increases death of retinal pigmented epithelium in geographic atrophy<sup>[22]</sup>. Previous works have confirmed that SINEs and SINE RNA regulate gene expression<sup>[23-25]</sup>. Our previous studies also indicated that murine SINE B1 antisense RNA retards the mouse aging process by removing accumulated ROS in senescent cells and regulating the expression of aging-associated genes<sup>[19]</sup>. Importantly, there are established methods for producing genetically engineered SINE RNAs that are of sufficient quality for cell and animal experiments<sup>[26-27]</sup>; the availability of these methods means that nucleic acid reagents of treating aged-related diseases can be obtained.

In this study, we examined whether human SINE antisense RNA (Aluas RNA) can protect human lens epithelial cells (HLECs) from apoptosis induced by MGO and sought to explore the mechanisms by which Aluas RNA could have this effect.

## MATERIALS AND METHODS

**Cell Culture and Cell Transfection** HLECs (SRA01/04, Huatuo, Suzhou, China) were cultured in DMEM medium (4.5 g/L glucose, ThermoFisher Scientific, USA), supplemented with 10% fetal calf serum (FCS; ZETA<sup>TM</sup> Life, USA) under 5% CO<sub>2</sub> at 37°C.

Yeast tRNA (tRNA) was purchased from Solarbio Life Sciences; Alu sense RNA (Alu RNA) and Alu antisense RNAs were prepared by our laboratory<sup>[26-27]</sup>. These Alu antisense RNAs include AluYas RNA, AluJBas RNA and AluSPas RNA. Our experiments have shown that all of them reduced the apoptosis of HLECs induced by MGO. Different Alu elements (AluY, AluJB and AluSP) have more than 80% homologous, thus we presented the results of AluYas RNA (Aluas RNA) in this manuscript. The Aluas RNA sequence (283 bp) is 5' – TGAGACGGAGTCTCGCTGTGTCGCCAGGCTGGAGTGCAGTGGCGGATCTCGGCTCACTGCAAGCTCCACCTCCAGGTTACGCCATTCTCCTGCCTCAGCCTCTTGAGTAGCTGGGACTACAGGCACCCGCCACCACACCCGGCTAATTTTTTTGCATTTTTAGTAGAGACGGGGTTTCACCGTATTAGCCAGGATGGTCTTGATCTCCTGACCTTGAT

CCGCCCACCTCGGCCTCCCAAAGTGCTGGGATTACAGGCGTGAGCCACCGCGCCCAGCC – 3'.

We compared the results of transfection of Aluas RNA into HLECs using Lipofectamine 2000 and calcium phosphate transfection (CPT)<sup>[28]</sup>. Although the transfection efficiency of Lipofectamine 2000 was relatively high, this method resulted in the death of a lot of HLECs. Transfection with CPT reagent had fewer side effects, and the transfection efficiency was also acceptable. We therefore used the CPT method to transfect tRNA, Alu RNA or Aluas RNA into HLECs. Briefly, 1.0×10<sup>5</sup> cells were plated in each well of 24-well plates, then cultured at 37°C for 24h. Fourteen microliters of transfection solution [72 μL of 1 mg/mL RNA, 28 μL of 0.5 mol/L calcium chloride, 54 μL of 2×HBS (280 mmol/L NaCl, 50 mmol/L HEPES, 1.5 mmol/L Na<sub>2</sub>HPO<sub>4</sub>, pH 7.05), and 856 μL double distilled water] was added to HLECs in one well of 24-well plate. Our subsequent experiments proved that 14 μL of the above formulation was the appropriate dose. CPT reagent alone was used as a negative control. Transfected HLECs were cultured for 48h under 5% CO<sub>2</sub> at 37°C. After 48h of transfection, the medium was replaced with fresh 10% FCS-DMEM medium. The cells were then treated with one of several concentrations of MGO: 0, 25, 50, 100, or 200 μmol/L (Shanghai Yuanye Bio-Technology Co. Ltd, China) for indicated time. The cells were harvested and used in later experiments.

**Cell Counting Kit-8 Assays** Cell counting kit-8 (CCK-8) (Boster Biological Technology, Wuhan, China) kit was used to assess HLEC viability according to the previous description<sup>[13]</sup>.

**Cell Viability/Death Detection** The Calcein-AM/PI double staining kit (BiolabTechnology Co., Ltd, Beijing, China) was used to detect the cell viability and cell death according to the description of Palsamy *et al*<sup>[29]</sup>.

**Reactive Oxygen Species Staining** Cytosolic ROS levels in HLECs were determined using a reactive species assay kit (Beyotime Biotechnology, Beijing, China) that uses the cell-permeant indicator molecule 2',7'-dichlorodihydrofluorescein diacetate (H<sub>2</sub>-DCFH-AD) according to the manufacturer's instructions and reported references<sup>[29-30]</sup>. One hundred cells were randomly selected from each sample, and the integral optical density (IOD) value of these one hundred cells was analyzed by Gel-Pro analyzer software. The total IOD values represent the fluorescence intensity of this sample. When comparing the effect of MGO concentration on ROS level, the intensity of fluorescence in the samples from the 0 μmol/L MGO group was set to 1; when comparing the effect of RNA on ROS levels, the intensity of fluorescence in CPT reagent+MGO group was set as 100%.

**Biochemical Analysis** Total-superoxide dismutase (T-SOD), glutathione peroxidase (GSH-Px), and malondialdehyde (MDA) kits (Shanghai Ruifen Biotechnology, Co., LTD,

China) were used to detect the activity of T-SOD, GSH-Px and levels of MDA, respectively, in the HLECs.

**Analysis of mRNA Expression Using RT-qPCR** TRIzol (Thermo Fisher Scientific) was used to extract total RNA from HLECs. RT-qPCR was performed according to previous description<sup>[19]</sup>. Alu RNA was detected using asymmetric RT-qPCR. Briefly, total RNA was extracted from HLECs using TRIzol and reverse transcribed into cDNA. The ratio of upstream primers to downstream primers of qPCR was 100:1; this method preferentially amplifies only Alu RNA. Table 1 presents the primers for RT-qPCR.

**Assessment of Apoptosis** Apoptosis was quantified using the annexin V-FITC method, which detects phosphatidyl serine that is externalized in the early phases of apoptosis, as described previously<sup>[31]</sup>.

**3-(4,5-Dimethylthiazol-2-yl)-2,5-diphenyltetrazolium Bromide Assays** HLECs were plated at  $2 \times 10^4$  per well in 96-well plates (200  $\mu$ L 10% FCS-DMEM), attached overnight, transfected with Aluas RNA, and treated with MGO. The viability of cells was measured using 3-(4,5-Dimethylthiazol-2-yl)-2,5-diphenyltetrazolium bromide assays (MTT) according to the previous description<sup>[13]</sup>.

**Western Blotting** HLECs were lysed in RIPA buffer (Beyotime Biotechnology, Shanghai, China) and stored at  $-80^\circ\text{C}$  until analysis. Protein levels were quantified using the BCA protein assay kit (Solarbio Life Sciences, China). The expression levels of protein were detected using Western blotting according to previous report<sup>[31]</sup>.

The intensity of each band was normalized to that of  $\beta$ -actin. The IOD value of each lane was analyzed using Gel-Pro analyzer software.

**Statistical Analysis** SPSS17.0 software was used for statistical processing of data when necessary. Differences between groups were analyzed by one-way ANOVA. Results are expressed as mean $\pm$ SD. Values were considered statistically significant when  $P < 0.05$ .

## RESULTS

**MGO Increases Cell Death, Cell Apoptosis and ROS Production in HLECs** To assay the effects of MGO on cell death, cell apoptosis and ROS production in HLECs, we treated HLECs with different concentrations of MGO (0, 25, 50, 100, or 200  $\mu$ mol/L). Treatment with MGO increased cell death, and almost no cell death was observed in HLECs that were treated without MGO (Figure 1A, 1B). MGO treatment also had a concentration-dependent growth inhibition effect in HLECs (Figure 1C) and induced significant production of ROS (Figure 1D). In contrast, no apparent ROS production was observed in HLECs that were treated without MGO (Figure 1D). Based on this, we sought to determine whether cell death induced by MGO reflected an increase in apoptosis.

**Table 1 Primers used for RT-qPCR**

Target	Sequences	Length of products (bp)
Nrf2	F: 5'-ACACGGTCCACAGCTCATC-3' R: 5'-TGCCTCCAAAGTATGTCAATCA-3'	96
Bax	F: 5'-CAGGATGCGTCCACCAAGAA-3' R: 5'-GCAAAGTAGAAGAGGGCAACCAC-3'	197
Bcl2	F: 5'-GCTACCGTCGTCGTGACTTCGC-3' R: 5'-CCCCACCGAACTCAAAGAAGG-3'	147
GSH-Px	F: 5'-GAAGTGC GAAGTGAATGG-3' R: 5'-TGTCGATGGTACGAAAGC-3'	224
$\gamma$ -GCS	F: 5'-TGGATGATGCCAACGAGTC-3' R: 5'-CCTAGTGAGCAGTACCACGAATA-3'	185
HO-1	F: 5'-GGGCTGTGAACTCTGTCCAAT-3' R: 5'-GGTGAGGGAAGTGTGTCAGG-3'	162
NQO1	F: 5'-TTCTGTGGCTTCCAGGTCTT-3' R: 5'-TCCAGACGTTTCTCCATCC-3'	104
Glo1	F: 5'-GCAGAACCGAGCCCCCGTC-3' R: 5'-GGATTAGCGTCATTCCAAGA-3'	172
Keap1	F: 5'-TACGATGTGGAACAGAGACGTGGA-3' R: 5'-ACAGGTACAGTTCGTGTTCAATCT-3'	264
Alu RNA	F: 5'-GGCTGGGCGGGTGGCTCAC-3' R: 5'-GTAGAGACGGGGTTCCACCG-3'	117
$\beta$ -actin	F: 5'-CCAACCGGAGAAAGATGA-3' R: 5'-CCAGAGGCGTACAGGGATAG-3'	97

F: Forward primer; R: Reverse primer.

Indeed, treatment with MGO induced HLEC apoptosis (Figure 1E).

Bearing in mind these results, we sought an optimal dose of MGO that would result in a moderate amount of cell damage for subsequent experiments. Exposure to 100  $\mu$ mol/L MGO caused 28.6% cell death (Figure 1B), 36.8% growth inhibition (Figure 1C), and 41.2% apoptosis (Figure 1E), compared to the appropriate controls, and induced robust ROS (Figure 1D). Therefore, we selected 100  $\mu$ mol/L MGO for subsequent experiments except where otherwise specified.

### Aluas RNA Rescues the Death of HLECs and Inhibits ROS Production Induced by MGO

To determine whether Aluas RNA can rescue HLEC death induced by MGO, we transfected HLECs with different RNAs, including Aluas RNA, Alu sense RNA (Alu RNA), tRNA, and CPT reagent and then added MGO at several concentrations (0, 25, 50, 100 and 200  $\mu$ mol/L) after 48h. MGO treatment decreased the viability of HLECs (Figure 2A). Aluas RNA transfection rescued HLEC viability after MGO treatment, but Alu RNA and tRNA did not (Figure 2A). We then examined whether Aluas RNA could rescue HLEC viability. Treatment with Aluas RNA was able to restore viability after MGO treatment (Figure 2B). These results suggest that while MGO reduces cell viability, Aluas RNA can protect cells against MGO-induced damage.

Compared to CPT reagent alone, Aluas RNA decreased cell death after treatment for 24h with 100  $\mu$ mol/L MGO (Figure 2C, 2D). The results show that Aluas RNA, but not Alu RNA,

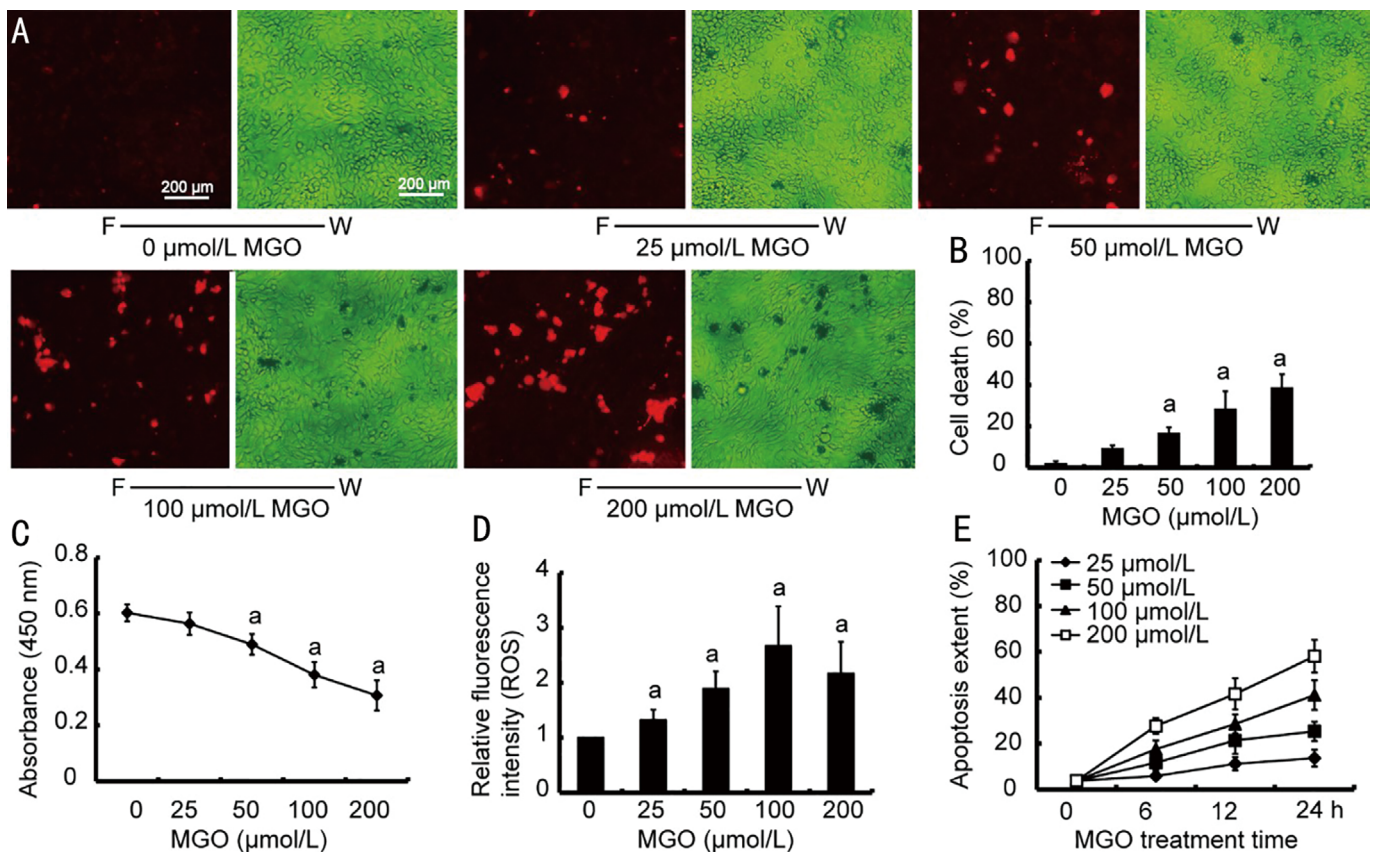


**Figure 1 MGO induces cell apoptosis and ROS production in HLECs** A: Images of PI staining for cell death in HLECs treated for 24h with different concentrations of MGO. F: Fluorescence; W: White light. B: Percentage of cell death measured from the images in Figure 1A.  $n=3$ .  $^{\ast}P<0.05$  vs 0 μmol/L MGO group. C: Measurement of HLEC proliferation *via* CCK-8 after treatment with MGO for 24h. Proliferation decreased significantly with increasing concentration of MGO. The proportion of growth inhibition induced by 100 μmol/L MGO was 36.8% (0.6025-0.3807/0.6025×100%). D: Relative fluorescence intensity (ROS) measured from images of the HLECs treated with the indicated concentrations of MGO for 24h. Fluorescence levels were corrected to account for the background. The intensity of fluorescence in cells treated with 0 μmol/L MGO was set to 1.  $^{\ast}P<0.05$  vs 0 μmol/L MGO group. E: MGO induces HLEC apoptosis. MGO: Methylglyoxal; HLEC: Human lens epithelial cells; CCK-8: Cell counting kit-8; ROS: Reactive oxygen species; PI: Propidium iodide.

tRNA, or appropriate experimental controls, rescued HLEC death induced by MGO.

Our previous studies indicated that murine SINE B1 antisense RNA could reduce ROS accumulation in the blood cells of senescent mice<sup>[19]</sup>. Therefore, we next investigated whether Aluas RNA inhibited ROS production in HLECs. We transfected HLECs with Aluas RNA, tRNA, or CPT reagent alone and then treated the cells with 100 μmol/L MGO for 24h. Transfection with Aluas RNA resulted in strong inhibition of the increased ROS production caused by MGO (Figure 2E). The intensity of fluorescence in CPT reagent+MGO group was set as 100%, the relative fluorescence intensities of Aluas RNA+MGO and tRNA+MGO groups were 21.31% and 87.6%, respectively (Figure 2F).

**Aluas RNA modulates the increase in Alu sense RNA (Alu RNA) induced by MGO** To determine whether Aluas RNA transfection affects the levels of Alu RNA, we used RT-qPCR to measure the levels of Alu RNA expression in HLECs. MGO treatment induced an increase in the Alu RNA expression level

(Figure 3). Aluas RNA transfection modulated the increase in Alu RNA induced by MGO (Figure 3).

**Aluas RNA Affects the Expression of Bcl-2 and Bax** Having previously observed that MGO induces apoptosis and that Aluas RNA can rescue cell death in the context of MGO treatment, we next sought to determine whether Aluas RNA affects HLEC apoptosis induced by MGO. Aluas RNA transfection inhibited apoptosis in HLECs. The fraction of apoptotic cells in the Aluas RNA+MGO group was lower than that of the MGO+CPT reagent group. To determine whether Aluas RNA affects apoptosis by modifying the levels of the anti-apoptotic factor and the pro-apoptotic factor, we then examined the relative expression of Bcl-2 and Bax mRNA and protein. MGO treatment increased Bax mRNA expression (Figure 4B) and protein expression (Figure 4C, 4D;  $P<0.05$ ) and decreased the Bcl-2 mRNA expression of (Figure 4E) and protein expression (Figure 4F, 4G;  $P<0.05$ ) compared to controls. However, treatment with Aluas RNA followed by treatment with 100 μmol/L MGO for 24h significantly

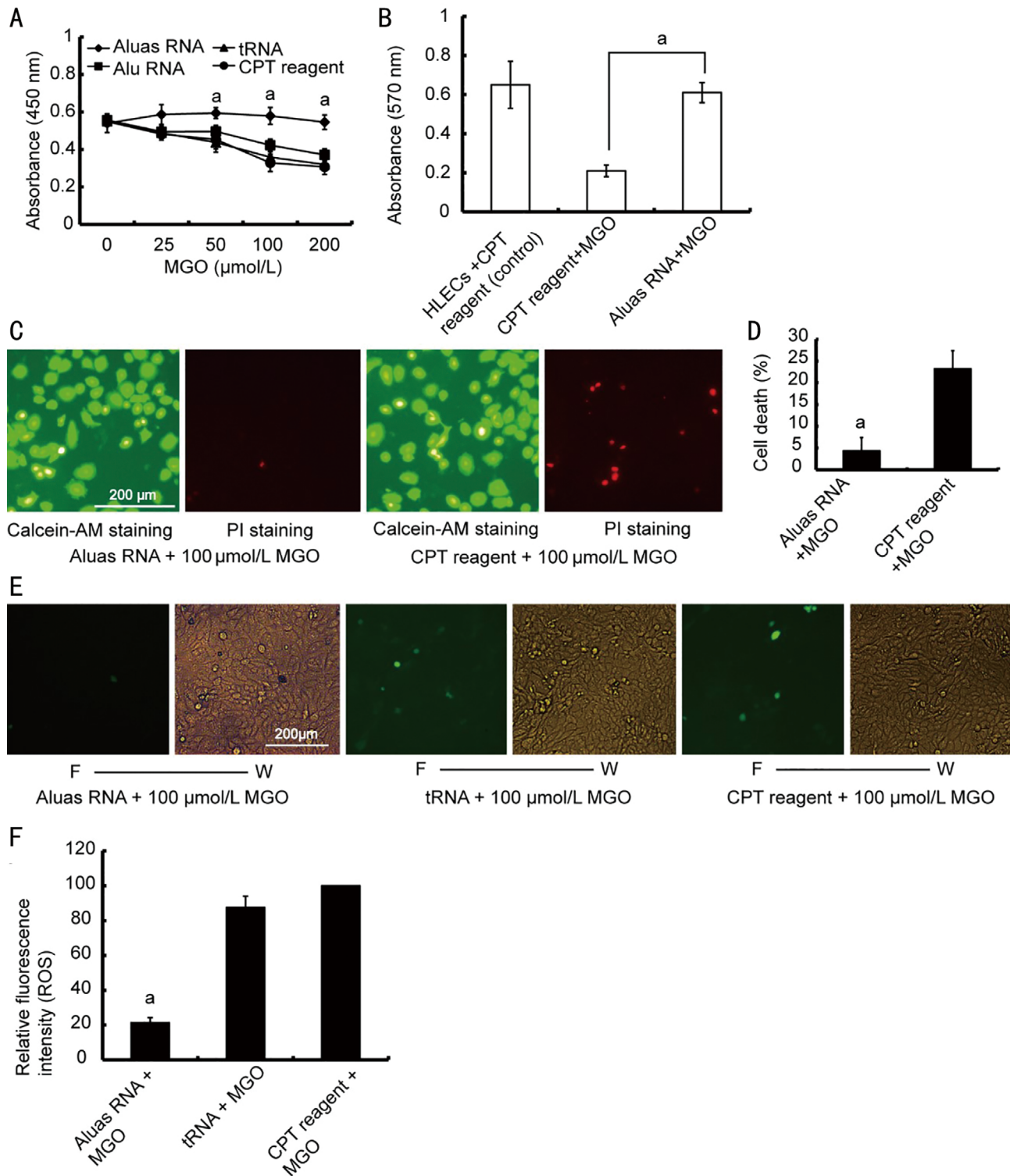


**Figure 2 Aluas RNA rescues HLEC death and inhibits ROS production induced by MGO** A: Detection of cell viability *via* CCK-8 in HLECs transfected with Aluas RNA, Alu RNA, tRNA or CPT reagent alone, with different concentrations of MGO. The proliferation of HLECs transfected with Aluas RNA was higher than that of HLECs transfected with Alu RNA, tRNA or CPT reagent alone. B: Detection of Aluas RNA effects on promoting the proliferation of HLECs using MTT assays. MGO reduces cell proliferation and reduces cell viability, while Aluas RNA protects cells against MGO-induced damage.  $n=3$ .  $^{\#}P<0.05$ . C: Images of calcein AM, showing live cells, and PI staining, showing cell death, in HLECs transfected with Aluas RNA and/or CPT reagent and treated with 100 μmol/L MGO for 24h. D: Calculation of cell death from the images shown in Figure 2C.  $n=3$ .  $^{\#}P<0.05$  vs CPT reagent + MGO group. E: Representative images of ROS levels in HLECs transfected with Aluas RNA, tRNA, or CPT reagent alone and treated with 100 μmol/L MGO. F: Fluorescence; W: White light. F: Relative fluorescence intensity of the images shown in Figure 2E. The intensity of fluorescence in the CPT reagent + MGO group was set to 100%. Fluorescence levels were corrected to account for image background.  $^{\#}P<0.05$  vs the tRNA + MGO group and the CPT reagent+MGO group. HLEC: Human lens epithelial cells; ROS: Reactive oxygen species; MGO: Methylglyoxal; CCK-8: Cell counting kit-8; CPT: Calcium phosphate transfection; MTT: 3-(4,5-Dimethylthiazol-2-yl)-2,5-diphenyltetrazolium bromide.

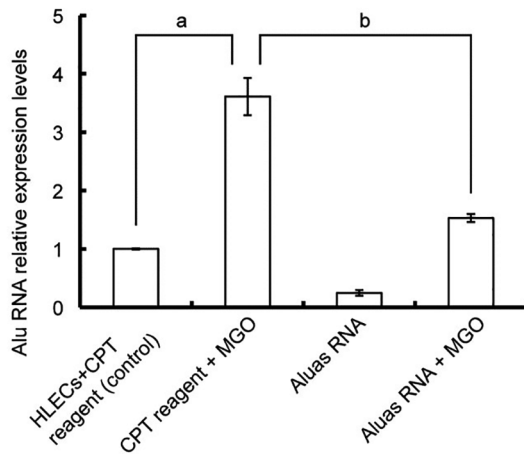


**Figure 3 Aluas RNA transfection inhibits the expression of Alu RNA** MGO treatment induces an increase in the expression level of Alu RNA. <sup>a</sup> $P < 0.05$ . Aluas RNA transfection inhibits the increase in Alu RNA induced by MGO. <sup>b</sup> $P < 0.05$ . <sup>a</sup>Statistical difference between the CPT reagent group and the CPT reagent + MGO group; <sup>b</sup>Statistical difference between the Aluas RNA+MGO group and the CPT reagent+MGO group. MGO: Methylglyoxal; CPT: Calcium phosphate transfection.

moderated both of these effects, inhibiting the increase in Bax mRNA expression (Figure 4B) and protein expression (Figure 4C, 4D;  $P < 0.05$ ) and the decrease in Bcl-2 mRNA expression (Figure 4E) and protein expression (Figure 4F, 4G;  $P < 0.05$ ).

### Aluas RNA Affects Oxidative Stress-Related Factors

Previous works demonstrated that MGO can cause oxidative stress in cells by scavenging superoxide dismutase (SOD)<sup>[32-33]</sup>; the resulting imbalance between the ROS generation and antioxidant defense leads to ROS accumulation, which can cause apoptosis<sup>[34]</sup>. To examine the role of oxidative stress in HLECs after MGO treatment, we next assessed the levels of T-SOD. Treatment with 100  $\mu\text{mol/L}$  MGO for 24h resulted in significantly lower T-SOD activity ( $P < 0.05$ ; Figure 5A) and GSH-Px activity ( $P < 0.05$ ; Figure 5B) compared to the HLECs without treatment with MGO. In contrast, treatment with Aluas RNA significantly rescued the MGO-induced decreases in T-SOD and GSH-Px ( $P < 0.05$ ; Figure 5A, 5B). MGO treatment for 24h also increased MDA content ( $P < 0.05$ ; Figure 5C), while Aluas RNA treatment reduced the MGO-induced increase in MDA content ( $P < 0.05$ ; Figure 5C). The results prove that Aluas RNA alleviates the oxidative stress induced by MGO in HLECs.

The glyoxalase system has important roles in reducing the toxicity of MGO<sup>[35]</sup>. Depletion of GSH can suppress Glo1 function and induce significant accumulation of MGO<sup>[36]</sup>. Totally 100  $\mu\text{mol/L}$  MGO treatment for 24h decreased the expression of Glo1 mRNA (Figure 5D). In contrast, treatment with Aluas RNA significantly rescued the MGO-induced decrease in Glo1 expression (Figure 5D).

### Aluas RNA Affects the Expression Levels of Genes of Nrf2 and Antioxidant Defense

A recent report illustrated the relationship between the Nrf2 pathway, a key pathway for dealing with oxidative stress, and cataracts. This report suggested that MGO can aggravate cataract formation by inhibiting Nrf2-dependent antioxidant protection<sup>[37]</sup>. We therefore examined whether Aluas RNA could affect the Nrf2 pathway. Treatment with 100  $\mu\text{mol/L}$  MGO for 24h decreased the expression of Nrf2 (Figure 6A), quinone oxidoreductase 1 (NQO1; Figure 6D), heme oxygenase 1 (HO-1; Figure 6E),  $\gamma$ -glutamylcysteine synthetase ( $\gamma$ -GCS; Figure 6F), and GSH-Px (Figure 6G) mRNA compared to control. In contrast, treatment with Aluas RNA significantly increased the levels of Nrf2 (Figure 6A), NQO1 (Figure 6D), HO-1 (Figure 6E),  $\gamma$ -GCS (Figure 6F), and GSH-Px (Figure 6G) mRNA compared to control ( $P < 0.05$ ). The levels of Nrf2 (Figure 6A), NQO1 (Figure 6D), HO-1 (Figure 6E),  $\gamma$ -GCS (Figure 6F), and GSH-Px (Figure 6G) mRNA were significantly increased in the Aluas RNA /MGO co-treated group compared to the MGO group ( $P < 0.05$ ). In addition, MGO treatment decreased the levels of Nrf2 protein (Figure 6B, 6C), and cotreatment with Aluas RNA and MGO significantly increased Nrf2 protein levels (Figure 6B, 6C).

MGO treatment induced greater Keap1 mRNA (Figure 6H) and protein expression (Figure 6I, 6J), while treatment with Aluas RNA followed by treatment with MGO significantly decreased Keap1 expression (Figure 6H-6J,  $P < 0.05$ ).

### Potential Mechanism for the Effect of Aluas RNA on MGO-Caused Apoptosis in HLECs

Based on the results above, we hypothesize that Aluas RNA reduces MGO-induced apoptosis of HLECs by enhancing antioxidant defense (Figure 7). Hwang *et al*<sup>[38]</sup> reported that  $\text{H}_2\text{O}_2$  induced Alu transcription and apoptosis in retinal pigment epithelial cells. Alu RNA accumulation causes P2X7 activation; P2X7 mediates influxes of  $\text{Ca}^{2+}$ , which is the key effector for ROS production from mitochondria<sup>[39]</sup>. Alu RNA expression promotes  $\text{Ca}^{2+}$  influx, in turn, couples the Pyk2/c-Src complex and PKC to initiate ERK1/2-directed mitochondrial stress. VDAC-1/2, the major channel at the outer mitochondrial membrane, is responsible for uptake of  $\text{Ca}^{2+}$  and ERK1/2 into mitochondria and promotes ROS production<sup>[39]</sup>. The accumulating ROS damages cellular proteins, lipids, DNA and other biological molecules and can cause cell apoptosis<sup>[40]</sup>. Our working hypothesis is that MGO induces Alu RNA expression, while the binding Aluas RNA with Alu RNA inhibits the resulting influx of  $\text{Ca}^{2+}$  and blocks toxic effects of Alu RNA. More experiments need to be performed in the future if we want to thoroughly prove the above hypothesis.

### DISCUSSION

Previous works have proved that MGO can cause cell

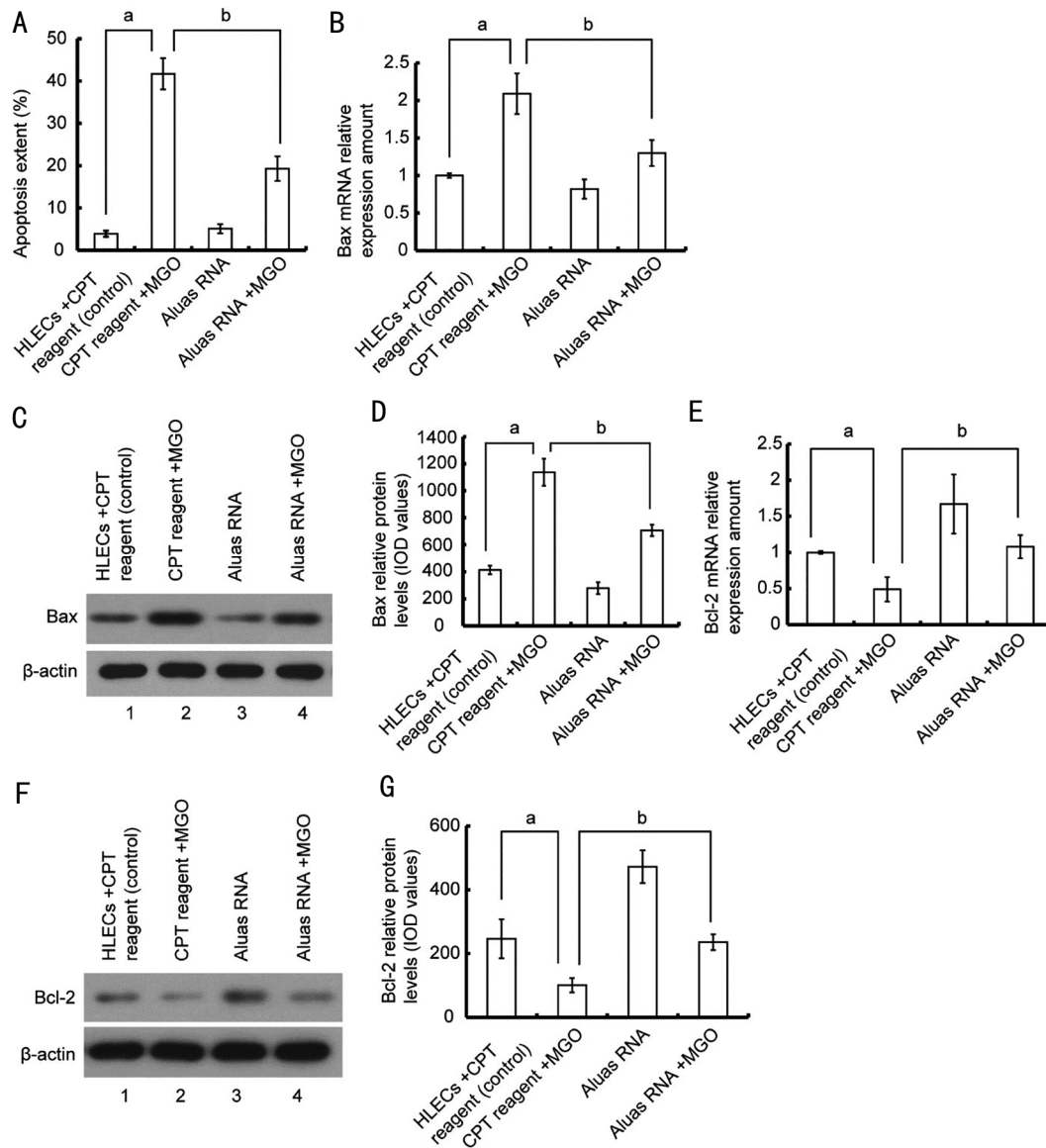


**Figure 4 Aluas RNA transfection ameliorates MGO-induced changes in Bax and Bcl-2 mRNA** A: Aluas RNA transfection inhibits MGO-induced apoptosis in HLECs. <sup>a</sup>*P*<0.05; <sup>b</sup>*P*<0.05. B: Aluas RNA inhibits the MGO-induced increase in Bax mRNA levels. <sup>a</sup>*P*<0.05; <sup>b</sup>*P*<0.05. C: Aluas RNA inhibits the MGO-induced increase in Bax protein levels. *n*=3. D: The amount of protein (IOD value) per lane for images shown in Figure 4C. <sup>a</sup>*P*<0.05; <sup>b</sup>*P*<0.05. E: Aluas RNA rescues the MGO-induced decrease in Bcl-2 mRNA levels. <sup>a</sup>*P*<0.05. <sup>b</sup>*P*<0.05. F: Aluas RNA rescues the MGO-induced decrease in Bcl-2 protein levels. *n*=3. G: The amount of protein (IOD value) per lane for images shown in Figure 4F. <sup>a</sup>Statistical difference between the CPT reagent group and the CPT reagent + MGO group; <sup>b</sup>Statistical difference between the Aluas RNA+MGO group and the CPT reagent +MGO group. MGO: Methylglyoxal; HLEC: Human lens epithelial cells; IOD: Integral optical density; CPT: Calcium phosphate transfection.

oxidative stress by scavenging SOD and glutathione<sup>[41-43]</sup>. The imbalance between ROS generation and antioxidant defense results in the ROS accumulation in cells, and accumulated ROS can damage cellular proteins, lipids, DNA and other biological molecules and cause cell apoptosis<sup>[33-34]</sup>. ROS accumulation causes human lens epithelial cells apoptosis, then lead to cataract formation. HLECs are immortalized cells that transition from an immortalized state to undergo apoptosis (loss of immortalization) when treated with MGO (or H<sub>2</sub>O<sub>2</sub>). In this way, there are some similarities in the molecular processes by which immortalized cells (HLECs) and primary

lens epithelial cells undergo apoptosis in response to oxidative damage. Therefore, HLECs treated with MGO can, to some extent, model the apoptosis induced by oxidative damage during the formation of cataracts.

It has also been reported that ROS account for MGO's role in inducing apoptosis<sup>[44-46]</sup>. In the present study, treatment with MGO increased HLEC death and apoptosis. These results are consistent with literature reports.

To begin to analyze the potential role of Aluas RNA in this process, we introduced Aluas RNA into HLECs by transfection. Interestingly, our results depended on the

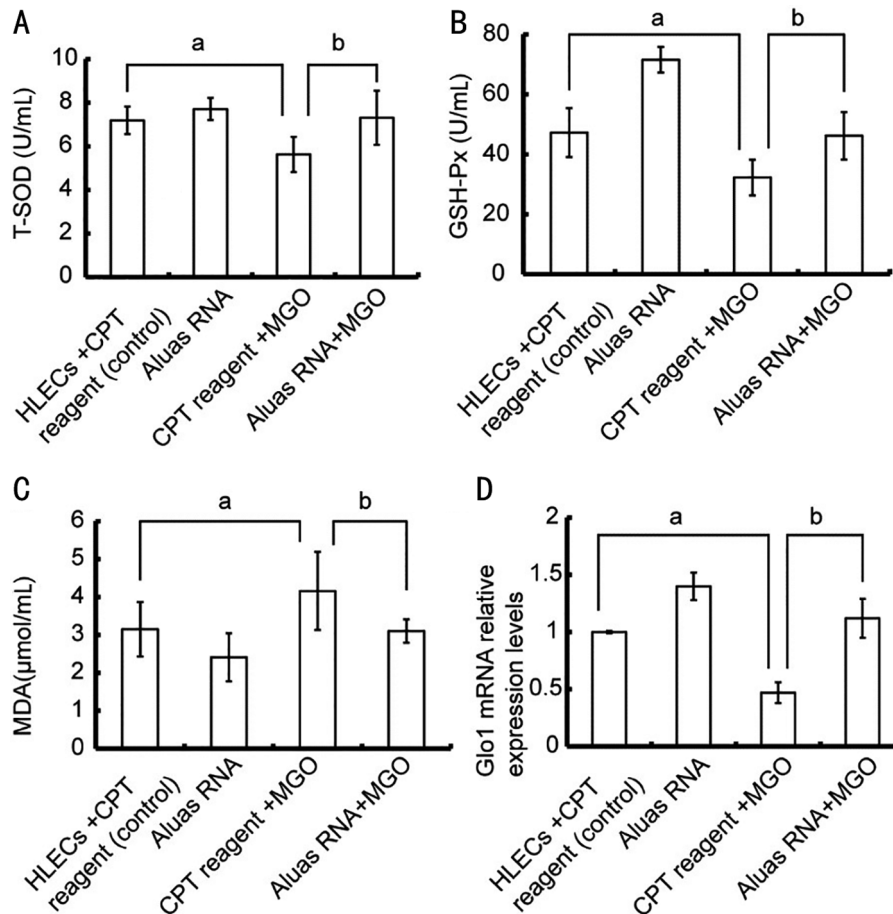


**Figure 5 Aluas RNA increased antioxidant protection in HLECs** A: Aluas RNA restores the MGO-dependent decrease in T-SOD activity in HLECs. <sup>a</sup> $P < 0.05$ ; <sup>b</sup> $P < 0.05$ . B: Aluas RNA partially rescues the MGO-dependent decrease in GSH-Px activity in HLECs. <sup>a</sup> $P < 0.05$ ; <sup>b</sup> $P < 0.05$ . C: Aluas RNA ameliorates the MGO-dependent increase in MDA content in HLECs. <sup>a</sup> $P < 0.05$ ; <sup>b</sup> $P < 0.05$ . D: Aluas RNA significantly rescues MGO-induced decreases in Glo1 expression. <sup>a</sup> $P < 0.05$ ; <sup>b</sup> $P < 0.05$ . <sup>a</sup>Statistical difference between the CPT reagent group and the CPT reagent + MGO group; <sup>b</sup>statistical difference between the Aluas RNA+MGO group and the CPT reagent +MGO group. MGO: Methylglyoxal; T-SOD: Total-superoxide dismutase; MDA: Malondialdehyde; CPT: Calcium phosphate transfection; HLEC: Human lens epithelial cells; GSH-Px: Glutathione peroxidase.

transfection method. We did not observe an anti-aging effect when Aluas RNA was transfected into human fibroblasts with Lipofectamine 2000. However, human fibroblasts transfected with Aluas RNA using CPT reagent did show a decrease in senescence (data not shown). We speculate that the anti-senescence effect of Aluas RNA is related not only to the RNA sequence but also to its position in the cells and fragment size. The RNAs generated by transfected expression vectors are normally located at transcriptional foci in the nucleus; however, the RNAs transfected using CPT reagent will first enter the cytoplasm and then enter into the nucleus, resulting in a more even distribution. In addition, the RNA fragments produced by transfected expression vectors are larger than those produced after transfection with CPT reagent. For our subsequent experiments, we therefore transfected HLECs with Aluas RNA using CPT reagent.

In this study, treatment with Aluas RNA rescued MGO-induced damage and increased proliferation in HLECs. It has been reported that SINE RNAs have important roles

in gene expression regulation<sup>[17]</sup>. Alu RNA accumulation activates the expression of apoptotic proteins and related to geographic atrophy, and an Alu RNA antisense oligonucleotide was recently reported to be effective for treating geographic atrophy<sup>[47-49]</sup>. We observed similar effects with MGO in HLECs; MGO treatment increased the expression level of Alu RNA, and Aluas RNA transfection inhibited this increase (Figure 3).

The most important factor in the development of cataracts is aging, though other factors such as environmental and genetic stresses are known to play a role<sup>[37]</sup>. One of the ways that aging contributes to the formation of cataracts is through the accumulation of oxidative damage. Indeed, aged eyes are more sensitive to ROS<sup>[50]</sup>, and lens epithelial cells have been reported to be sensitive to ROS<sup>[51-52]</sup>. In this study, transfection with Aluas RNA restored MGO-induced increases in ROS levels, and rescued MGO-induced decreases in the activities of T-SOD and GSH-Px, which are associated with antioxidant defense. Aluas RNA treatment also increased the expression

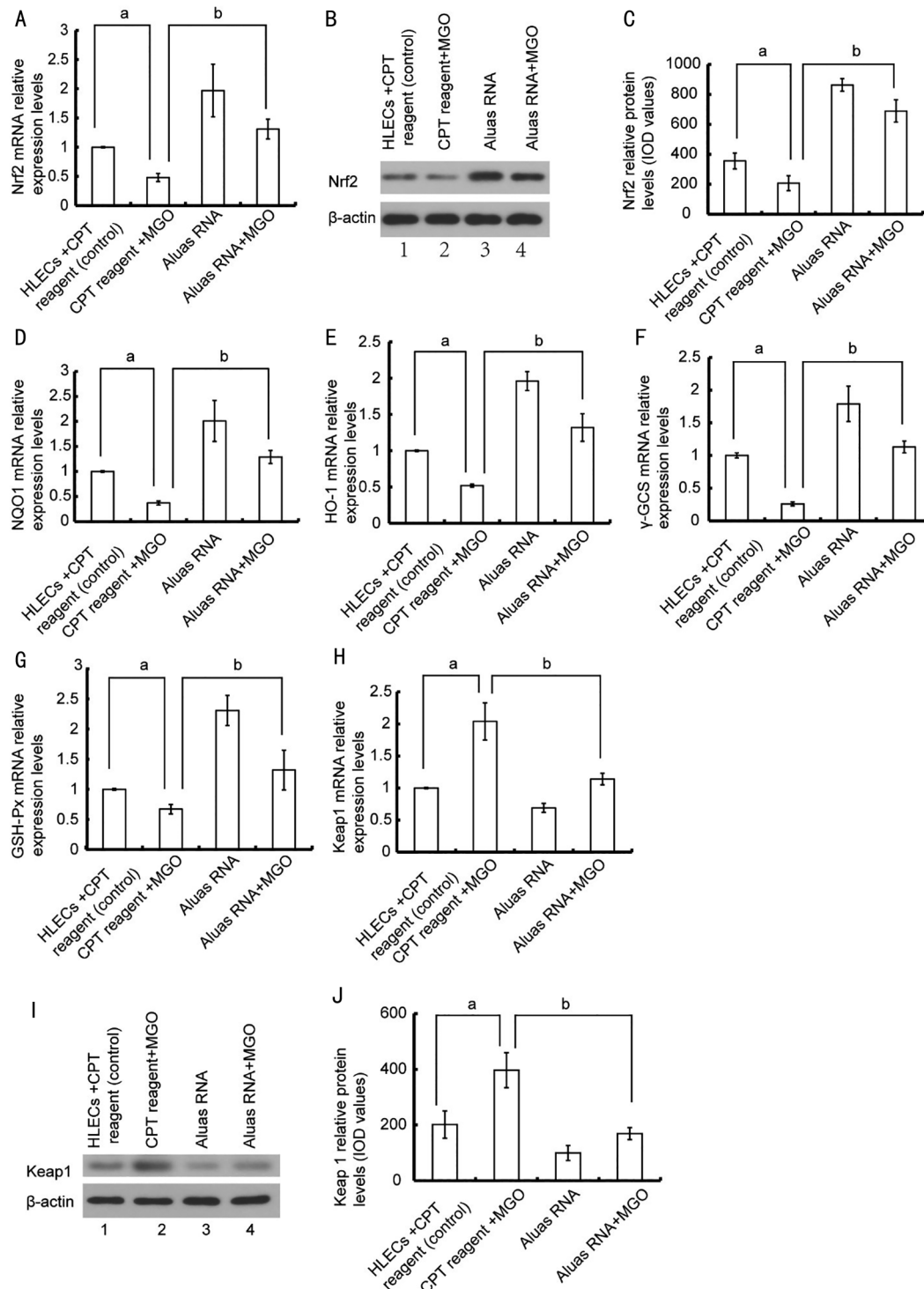


**Figure 6 Aluas RNA increases the expression of Nrf2 and antioxidant defense mRNAs** A: Aluas RNA rescues the MGO-induced down-regulation of Nrf2 mRNA level. <sup>a</sup>*P*<0.05; <sup>b</sup>*P*<0.05. B: Aluas RNA rescues the MGO-induced down-regulation of Nrf2 protein expression. C: The amount of protein (IOD value) per lane shown in Figure 6B (means of three independent experiments). <sup>a</sup>*P*<0.05; <sup>b</sup>*P*<0.05. D: Aluas RNA rescues the MGO-induced down-regulation of NQO1 mRNA. <sup>a</sup>*P*<0.05; <sup>b</sup>*P*<0.05. E: Aluas RNA rescues the MGO-induced down-regulation of HO-1 mRNA. <sup>a</sup>*P*<0.05; <sup>b</sup>*P*<0.05. F: Aluas RNA rescues the MGO-induced down-regulation of  $\gamma$ -GCS mRNA level. <sup>a</sup>*P*<0.05; <sup>b</sup>*P*<0.05. G: Aluas RNA rescues the MGO-induced down-regulation of GSH-Px mRNA. <sup>a</sup>*P*<0.05; <sup>b</sup>*P*<0.05. H: Aluas RNA rescues the MGO-induced up-regulation of Keap1 mRNA level. <sup>a</sup>*P*<0.05; <sup>b</sup>*P*<0.05. I: Aluas RNA rescues the MGO-induced up-regulation of Keap1 protein. *n*=3. J: The amount of protein (IOD value) per lane shown in Figure 6I. <sup>a</sup>*P*<0.05; <sup>b</sup>*P*<0.05. <sup>a</sup>Statistical difference between the CPT reagent group and the CPT reagent + MGO group; <sup>b</sup>Statistical difference between the Aluas RNA+MGO group and the CPT reagent + MGO group. MGO: Methylglyoxal; IOD: Integral optical density;  $\gamma$ -GCS:  $\gamma$ -glutamylcysteine synthetase; GSH-Px: Glutathione peroxidase; CPT: Calcium phosphate transfection.

of Glo1 mRNA (Figure 4). The glyoxalase system has an important role in reducing toxicity of MGO<sup>[53]</sup>. Depletion of

GSH suppresses the Glo1 function and induces significant MGO accumulation<sup>[54]</sup>.

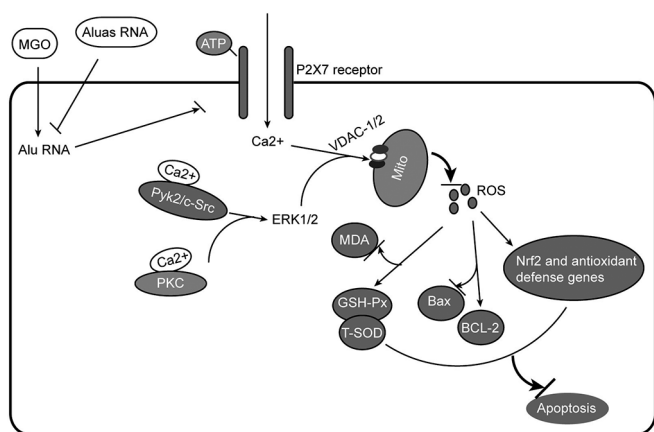


**Figure 7 Potential mechanism of Aluas RNA action in MGO-induced apoptosis of HLECs** MGO treatment increases Alu RNA level in HLECs. Alu RNA in turn mediates an influx of  $Ca^{2+}$ , which activates P2X7 and serves as the key effector for ROS production from mitochondria.  $Ca^{2+}$  influx couples the Pyk2/c-Src complex and PKC to initiate ERK1/2-directed mitochondrial stress. VDAC-1/2, the major channel at outer mitochondrial membrane, is also responsible for uptake of  $Ca^{2+}$  and ERK1/2 into mitochondria for ROS production. Aluas RNA transfection inhibits the MGO-induced increase in Alu RNA levels, inhibiting ROS production, restoring the activity of T-SOD and GSH-Px, and moderating the MDA content increase after MGO treatment. In addition, Aluas RNA significantly restored the MGO-induced down-regulation of Nrf2 and antioxidant defense genes. Mito: mitochondria. MGO: Methylglyoxal; HLEC: Human lens epithelial cells; ROS: Reactive oxygen species; T-SOD: Total-superoxide dismatase; GSH-Px: Glutathione peroxidase; MDA: Malondialdehyde.

Several reports have proved that MGO induces apoptosis in cells, including HK-2 cells<sup>[55]</sup>, rat INS-1 pancreatic  $\beta$ -cells<sup>[56]</sup> and human retinal pigment epithelial cells<sup>[57]</sup>. Our results confirmed that MGO can also induce apoptosis in HLECs. Aluas RNA also decreased Bax, the pro-apoptotic factor and increased Bcl-2, the anti-apoptotic factor. These results suggest that Aluas RNA alleviates oxidative stress and inhibits apoptosis in HLECs cells exposed to MGO. The target sequences of (sense) human Alu RNA interact with proteins of the signal recognition particle and regulate gene expression by binding to a protein to initiate the apoptotic pathway<sup>[58-59]</sup>. We speculate that the Aluas RNA plays a role in ameliorating apoptosis by binding to Alu RNA and counteracting its pro-apoptotic activity.

Nrf2 works as a molecular switch for the Nrf2-mediated antioxidant systems<sup>[60]</sup>. Nrf2 is a vital inducer of nuclear transcription<sup>[61]</sup> that controls the transcription of many antioxidant genes<sup>[62]</sup>. In this way, Nrf2 is the most important endogenous antioxidant stress pathway<sup>[63-64]</sup>. Recent reports have illustrated a relationship between Nrf2 and cataracts<sup>[37]</sup>. MGO was reported to be an inhibitor of Nrf2 suppressors, and one study indicated that MGO can aggravate cataract formation

via suppressing Nrf2-dependent antioxidant protection<sup>[35]</sup>. These reports suggest that Nrf2 is an important target for preventing and delaying cataract formation. MGO induced overproduction of ROS that damages lens constituents and induces failure of the Nrf2 dependent cytoprotein<sup>[65]</sup>. Keap1 is the negative regulator of Nrf2<sup>[5]</sup>. The results here proved that MGO induced the high expression of Keap1 and decreased Nrf2 expression, which was consistent with the reports of Palsamy *et al*<sup>[65]</sup>. In addition, Aluas RNA treatment increased Nrf2 expression and decreased Keap1 expression (Figure 6).

To examine whether Aluas RNA activates the antioxidant defense genes to restrain the apoptosis induced by MGO, we examined the mRNA levels of GSH-Px, HO-1,  $\gamma$ -GCS and NQO1 genes. These results proved that the mRNA levels of GSH-Px, HO-1,  $\gamma$ -GCS and NQO1 (antioxidant defense genes) were all decreased after MGO treatment. Our results confirmed that MGO inhibits the Nrf2 and reduces the expression of relevant antioxidant factors. The loss of these antioxidants, in turn, leaves HLECs cells less able to remove the MGO-induced ROS, which in turn causes oxidative damage and induces apoptosis. Co-treatment with Aluas RNA significantly increases Nrf2 mRNA and protein levels and mRNA levels of GSH-Px, HO-1, NQO1 and  $\gamma$ -GCS genes. This is consistent with the hypothesis that Aluas RNA activates Nrf2 *via* increasing the expression of GSH-Px, HO-1, NQO1 and  $\gamma$ -GCS—among the most important antioxidant enzymes, improving responses to oxidative stress, maintaining redox balance, and reducing MGO-induced cell apoptosis.

In summary, we outline the possible molecular mechanisms (Figure 7) that Aluas RNA ameliorates MGO-induced apoptosis of human HLECs in combination with the reported literature and our results in this study. The results in this study treatment with Aluas RNA can alleviate MGO-induced oxidative damage and apoptosis in HLECs. Our evidence further suggests that Aluas RNA decreases apoptosis by inhibiting Alu RNA levels, then by increasing the antioxidant activity and by activating the expression of Nrf2 and antioxidant defense genes.

#### ACKNOWLEDGEMENTS

**Authors' contributions:** Wang XF and Yan LF designed the experiments and wrote the manuscript; Wu PY, Ji N, Wu CG, Wang XD, and Liu X performed the experiments; Song ZX, Khan M, Shah S, and Du YH analyzed the data. All authors reviewed and approved the final manuscript for submission.

**Foundations:** Supported by the National Natural Science Foundation of China (No.81771499); the Natural Science Foundation of Hebei Province, China (No.H2018206099; No.H2021206460).

**Conflicts of Interest:** Wu PY, None; Ji N, None; Wu CG, None; Wang XD, None; Liu X, None; Song ZX, None; Khan

**M**, None; **Shah S**, None; **Du YH**, None; **Wang XF**, None; **Yan LF**, None.

#### REFERENCES

- 1 Hosseini H, Teimouri M, Shabani M, Koushki M, Babaei Khorzoughi R, Namvarjah F, Izadi P, Meshkani R. Resveratrol alleviates non-alcoholic fatty liver disease through epigenetic modification of the Nrf2 signaling pathway. *Int J Biochem Cell Biol* 2020;119:105667.
- 2 Di Domenico F, Lanzillotta C. The disturbance of protein synthesis/degradation homeostasis is a common trait of age-related neurodegenerative disorders. *Adv Protein Chem Struct Biol* 2022;132:49-87.
- 3 Zhang SX, Ma JH, Bhatta M, Fliesler SJ, Wang JJ. The unfolded protein response in retinal vascular diseases: implications and therapeutic potential beyond protein folding. *Prog Retin Eye Res* 2015;45:111-131.
- 4 Cullinan SB, Alan Diehl J. PERK-dependent activation of Nrf2 contributes to redox homeostasis and cell survival following endoplasmic reticulum stress. *J Biol Chem* 2004;279(19):20108-20117.
- 5 Cullinan SB, Alan Diehl J. Coordination of ER and oxidative stress signaling: the PERK/Nrf2 signaling pathway. *Int J Biochem Cell Biol* 2006;38(3):317-332.
- 6 Kensler TW, Wakabayashi N, Biswal S. Cell survival responses to environmental stresses via the Keap1-Nrf2-ARE pathway. *Annu Rev Pharmacol Toxicol* 2007;47:89-116.
- 7 Sadeghiani G, Khanezhad M, Sadighi Gilani MA, Amidi F, Malekzadeh M, Rastegar T. Evaluation of Nrf2/ARE signaling pathway in the presence of pentoxifylline as a cryoprotectant in mouse spermatogonial stem cells. *Biopreserv Biobank* 2022.
- 8 Taguchi K, Motohashi H, Yamamoto M. Molecular mechanisms of the Keap1-Nrf2 pathway in stress response and cancer evolution. *Genes Cells* 2011;16(2):123-140.
- 9 Sanchez C, Zappia J, Lambert C, Foguene J, Dierckxsens Y, Dubuc JE, Delcour JP, Gothot A, Henrotin Y. *Curcuma longa* and *Boswellia serrata* extracts modulate different and complementary pathways on human chondrocytes in vitro: deciphering of a transcriptomic study. *Front Pharmacol* 2022;13:931914.
- 10 Enomoto A, Itoh K, Nagayoshi E, Haruta J, Kimura T, O'Connor T, Harada T, Yamamoto M. High sensitivity of Nrf2 knockout mice to acetaminophen hepatotoxicity associated with decreased expression of ARE-regulated drug metabolizing enzymes and antioxidant genes. *Toxicol Sci* 2001;59(1):169-177.
- 11 Lee JM, Calkins MJ, Chan KM, Kan YW, Johnson JA. Identification of the NF-E2-related factor-2-dependent genes conferring protection against oxidative stress in primary cortical astrocytes using oligonucleotide microarray analysis. *J Biol Chem* 2003;278(14):12029-12038.
- 12 Kwak MK, Kensler TW, Casero RA Jr. Induction of phase 2 enzymes by serum oxidized polyamines through activation of Nrf2: effect of the polyamine metabolite acrolein. *Biochem Biophys Res Commun* 2003;305(3):662-670.
- 13 Ma Y, Liu F, Xu YL. Protective effect of  $\beta$ -glucogallin on damaged cataract against methylglyoxal induced oxidative stress in cultured lens epithelial cells. *Med Sci Monit* 2019;25:9310-9318.
- 14 Prisco SZ, Hartweck L, Keen JL, Vogel N, Kazmirczak F, Eklund M, Hemnes AR, Brittain EL, Prins KW. Glyoxylase-1 combats dicarbonyl stress and right ventricular dysfunction in rodent pulmonary arterial hypertension. *Front Cardiovasc Med* 2022;9:940932.
- 15 Long X, He NM, Tan LX, Yang YH, Zhou JP, Liu ZY, Mo MH, Liu T. Methylglyoxal has different impacts on the fungistatic roles of ammonia and benzaldehyde, and lactoylglutathione lyase is necessary for the resistance of *Arthrobotrys oligospora* to soil fungistasis. *Front Cell Infect Microbiol* 2021;11:640823.
- 16 Bungau S, Abdel-Daim MM, Tit DM, Ghanem E, Sato S, Maruyama-Inoue M, Yamane S, Kadonosono K. Health benefits of polyphenols and carotenoids in age-related eye diseases. *Oxid Med Cell Longev* 2019;2019:9783429.
- 17 Wang XF, Ma ZH, Cheng JJ, Lv ZJ. A genetic program theory of aging using an RNA population model. *Ageing Res Rev* 2014;13:46-54.
- 18 Kosushkin SA, Ustyantsev IG, Borodulina OR, Vassetzky NS, Kramerov DA. Tail wags dog's SINE: retropositional mechanisms of can SINE depend on its A-tail structure. *Biology* 2022;11(10):1403.
- 19 Song ZX, Shah S, Lv BX, Ji N, Liu X, Yan LF, Khan M, Zhao YF, Wu PY, Liu SF, Zheng L, Su LB, Wang XF, Lv ZJ. Anti-aging and anti-oxidant activities of murine short interspersed nuclear element antisense RNA. *Eur J Pharmacol* 2021;912:174577.
- 20 Ivanova E, Berger A, Scherrer A, Alkalaeva E, Strub K. Alu RNA regulates the cellular pool of active ribosomes by targeted delivery of SRP9/14 to 40S subunits. *Nucleic Acids Res* 2015;43(5):2874-2887.
- 21 Berger A, Ivanova E, Gareau C, Scherrer A, Mazroui R, Strub K. Direct binding of the Alu binding protein dimer SRP9/14 to 40S ribosomal subunits promotes stress granule formation and is regulated by Alu RNA. *Nucleic Acids Res* 2014;42(17):11203-11217.
- 22 Yoshida H, Matsushita T, Kimura E, Fujita Y, Keany R, Ikeda T, Toshimori M, Imanaka T, Nakamura M. Systemic expression of Alu RNA in patients with geographic atrophy secondary to age-related macular degeneration. *PLoS One* 2019;14(8):e0220887.
- 23 Ma ZH, Kong XL, Liu SF, Yin SX, Zhao YH, Liu C, Lv ZJ, Wang XF. Combined sense-antisense Alu elements activate the *EGFP* reporter gene when stable transfection. *Mol Genet Genomics* 2017;292(4):833-846.
- 24 Wang XF, Ma ZH, Kong XL, Lv ZJ. Effects of RNAs on chromatin accessibility and gene expression suggest RNA-mediated activation. *Int J Biochem Cell Biol* 2016;79:24-32.
- 25 Zhang XO, Pratt H, Weng ZP. Investigating the potential roles of SINEs in the human genome. *Annu Rev Genomics Hum Genet* 2021;22:199-218.
- 26 Liu C, Zhao YH, Yin SX, Liu SF, Zhang HL, Wang XF, Lv ZJ. The expression and construction of engineering *Escherichia coli* producing humanized AluY RNAs. *Microb Cell Fact* 2017;16(1):183.
- 27 Khan M, Yan LF, Lv BX, Ji N, Shah S, Liu X, Song ZX, Zhao YF, Wang XF, Lv ZJ. The preparation of endotoxin-free

- genetically engineered murine B1 antisense RNA. *Anal Biochem* 2020;599:113737.
- 28 Kwon M, Firestein BL. DNA transfection: calcium phosphate method. *Methods Mol Biol* 2013;1018:107-110.
- 29 Palsamy P, Ayaki M, Elanchezhian R, Shinohara T. Promoter demethylation of *Keap1* gene in human diabetic cataractous lenses. *Biochem Biophys Res Commun* 2012;423(3):542-548.
- 30 Elanchezhian R, Palsamy P, Madson CJ, Lynch DW, Shinohara T. Age-related cataracts: homocysteine coupled endoplasmic reticulum stress and suppression of Nrf2-dependent antioxidant protection. *Chem Biol Interact* 2012;200(1):1-10.
- 31 Wang XF, Witting PK, Salvatore BA, Neuzil J. Vitamin E analogs trigger apoptosis in HER2/erbB2-overexpressing breast cancer cells by signaling via the mitochondrial pathway. *Biochem Biophys Res Commun* 2005;326(2):282-289.
- 32 Suantawee T, Thilavech T, Cheng H, Adisakwattana S. Cyanidin attenuates methylglyoxal-induced oxidative stress and apoptosis in INS-1 pancreatic  $\beta$ -cells by increasing glyoxalase-1 activity. *Nutrients* 2020;12(5):1319.
- 33 Khan MA, Anwar S, Aljarbou AN, Al-Orainy M, Aldebasi YH, Islam S, Younus H. Protective effect of thymoquinone on glucose or methylglyoxal-induced glycation of superoxide dismutase. *Int J Biol Macromol* 2014;65:16-20.
- 34 Do MH, Lee JH, Ahn J, Hong MJ, Kim J, Kim SY. Isosamidin from *Peucedanum japonicum* roots prevents methylglyoxal-induced glucotoxicity in human umbilical vein endothelial cells via suppression of ROS-mediated bax/bcl-2. *Antioxidants (Basel)* 2020;9(6):531.
- 35 Wang ZW, Zhao D, Chen L, Li JJ, Yuan GH, Yang GS, Zhang H, Guo XH, Zhang JQ. Glycine increases glyoxalase-1 function by promoting nuclear factor erythroid 2-related factor 2 translocation into the nucleus of kidney cells of streptozotocin-induced diabetic rats. *J Diabetes Invest* 2019;10(5):1189-1198.
- 36 de Oliveira MR, de Souza ICC, Fürstenau CR. Promotion of mitochondrial protection by naringenin in methylglyoxal-treated SH-SY5Y cells: involvement of the Nrf2/GSH axis. *Chem Biol Interact* 2019;310:108728.
- 37 Liu XF, Hao JL, Xie T, Malik TH, Lu CB, Liu C, Shu C, Lu CW, Zhou DD. Nrf2 as a target for prevention of age-related and diabetic cataracts by against oxidative stress. *Aging Cell* 2017;16(5):934-942.
- 38 Hwang YE, Baek YM, Baek A, Kim DE. Oxidative stress causes Alu RNA accumulation via PIWIL4 sequestration into stress granules. *BMB Rep* 2019;52(3):196-201.
- 39 Mao XY, Fang WY, Liu QH. An emerging role of Alu RNA in geographic atrophy pathogenesis: the implication for novel therapeutic strategies. *Discov Med* 2016;22(123):337-349.
- 40 Zuo XY, Ren SX, Zhang H, Tian JF, Tian RN, Han B, Liu H, Dong Q, Wang ZY, Cui YF, Niu R, Zhang F. Chemotherapy induces ACE2 expression in breast cancer via the ROS-AKT-HIF-1 $\alpha$  signaling pathway: a potential prognostic marker for breast cancer patients receiving chemotherapy. *J Transl Med* 2022;20(1):509.
- 41 Oliveira AL, Medeiros ML, de Oliveira MG, Teixeira CJ, Mónica FZ, Antunes E. Enhanced RAGE expression and excess reactive-oxygen species production mediates rho kinase-dependent detrusor overactivity after methylglyoxal exposure. *Front Physiol* 2022;13:860342.
- 42 Darenskaya M, Chugunova E, Kolesnikov S, Semenova N, Michalevich I, Nikitina O, Lesnaya A, Kolesnikova L. Receiver operator characteristic (ROC) analysis of lipids, proteins, dna oxidative damage, and antioxidant defense in plasma and erythrocytes of young reproductive-age men with early stages of type 1 diabetes mellitus (T1DM) nephropathy in the irkutsk region, russia. *Metabolites* 2022;12(12):1282.
- 43 Schalkwijk CG, Stehouwer CDA. Methylglyoxal, a highly reactive dicarbonyl compound, in diabetes, its vascular complications, and other age-related diseases. *Physiol Rev* 2020; 100(1): 407-461.
- 44 Chen W, Zhang H, Liu GS, Kang J, Wang B, Wang J, Li J, Wang H. Lutein attenuated methylglyoxal-induced oxidative damage and apoptosis in PC12 cells via the PI3K/Akt signaling pathway. *J Food Biochem* 2022;46(12):e14382.
- 45 Liu D, Cheng Y, Tang ZP, Chen JL, Xia Y, Xu CB, Cao XY. Potential mechanisms of methylglyoxal-induced human embryonic kidney cells damage: regulation of oxidative stress, DNA damage, and apoptosis. *Chem Biodivers* 2022;19(2):e202100829.
- 46 Wang G, Wang YN, Yang QZ, Xu CR, Zheng YK, Wang LQ, Wu JB, Zeng M, Luo M. Metformin prevents methylglyoxal-induced apoptosis by suppressing oxidative stress *in vitro* and *in vivo*. *Cell Death Dis* 2022;13(1):29.
- 47 Kaarniranta K, Pawlowska E, Szczepanska J, Blasiak J. DICER1 in the pathogenesis of age-related macular degeneration (AMD) - *Alu* RNA accumulation versus miRNA dysregulation. *Aging Dis* 2020;11(4):851-862.
- 48 Yamada K, Kaneko H, Shimizu H, Suzumura A, Namba R, Takayama K, Ito S, Sugimoto M, Terasaki H. Lamivudine inhibits *Alu* RNA-induced retinal pigment epithelium degeneration via anti-inflammatory and anti-senescence activities. *Transl Vis Sci Technol* 2020;9(8):1.
- 49 Shiromoto Y, Sakurai M, Qu H, Kossenkov AV, Nishikura K. Processing of *Alu* small RNAs by DICER/ADAR1 complexes and their RNAi targets. *RNA* 2020;26(12):1801-1814.
- 50 Babizhayev MA, Yegorov YE. Reactive oxygen species and the aging eye: specific role of metabolically active mitochondria in maintaining lens function and in the initiation of the oxidation-induced maturity onset cataract—a novel platform of mitochondria-targeted antioxidants with broad therapeutic potential for redox regulation and detoxification of oxidants in eye diseases. *Am J Ther* 2016;23(1):e98-e117.
- 51 Ahmad A, Ahsan H. Biomarkers of inflammation and oxidative stress in ophthalmic disorders. *J Immunoassay Immunochem* 2020;41(3):257-271.
- 52 Ye W, Ma JY, Wang F, Wu T, He MM, Li J, Pei R, Zhang LN, Wang YF, Zhou J. LncRNA *MALAT1* regulates miR-144-3p to facilitate epithelial-mesenchymal transition of lens epithelial cells via the ROS/NRF2/Notch1/snail pathway. *Oxid Med Cell Longev* 2020;2020:8184314.

- 53 Wang J, Yang X, Wang Z, Wang J. Role of the glyoxalase system in breast cancer and gynecological cancer-implications for therapeutic intervention: a review. *Front Oncol* 2022;12:857746.
- 54 Yang CT, Meng FH, Chen L, Li X, Cen LJ, Wen YH, Li CC, Zhang H. Inhibition of methylglyoxal-induced ages/rage expression contributes to dermal protection by n-acetyl-l-cysteine. *Cell Physiol Biochem* 2017;41(2):742-754.
- 55 Park SH, Choi HI, Ahn J, Jang YJ, Ha TY, Seo HD, Kim YS, Lee DH, Jung CH. Autophagy functions to prevent methylglyoxal-induced apoptosis in HK-2 cells. *Oxid Med Cell Longev* 2020;2020:8340695.
- 56 Liu CX, Huang YH, Zhang YF, Chen XR, Kong X, Dong Y. Intracellular methylglyoxal induces oxidative damage to pancreatic beta cell line INS-1 cell through Ire1 $\alpha$ -JNK and mitochondrial apoptotic pathway. *Free Radic Res* 2017;51(4):337-350.
- 57 Pyun BJ, Kim YS, Lee IS, Jung DH, Kim JH, Kim JS. *Osteomeles schwerinae* extract and its major compounds inhibit methylglyoxal-induced apoptosis in human retinal pigment epithelial cells. *Molecules* 2020;25(11):2605.
- 58 Di Ruocco F, Basso V, Rivoire M, Mehlen P, Ambati J, De Falco S, Tarallo V. Alu RNA accumulation induces epithelial-to-mesenchymal transition by modulating miR-566 and is associated with cancer progression. *Oncogene* 2018;37(5):627-637.
- 59 Baryakin DN, Semenov DV, Savelyeva AV, Koval OA, Rabinov IV, Kuligina EV, Richter VA. Alu- and 7SL RNA analogues suppress MCF-7 cell viability through modulating the transcription of endoplasmic reticulum stress response genes. *Acta Naturae* 2013;5(4):83-93.
- 60 Gong YF, Yang Y. Activation of Nrf2/AREs-mediated antioxidant signalling, and suppression of profibrotic TGF- $\beta$ 1/Smad3 pathway: a promising therapeutic strategy for hepatic fibrosis—a review. *Life Sci* 2020;256:117909.
- 61 Michaličková D, Hrnčíř T, Canová NK, Slanař O. Targeting Keap1/Nrf2/ARE signaling pathway in multiple sclerosis. *Eur J Pharmacol* 2020;873:172973.
- 62 Ajuwon OR, Marnewick JL, Oguntibeju OO, Davids LM. Red palm oil ameliorates oxidative challenge and inflammatory responses associated with lipopolysaccharide-induced hepatic injury by modulating NF- $\kappa$ B and Nrf2/GCL/HO-1 signaling pathways in rats. *Antioxidants (Basel)* 2022;11(8):1629.
- 63 Su YY, Xu JQ, Chen SQ, Feng JX, Li JC, Lei ZH, Qiao LY, Wang YN, Zeng DW. Astragaloside IV protects against ischemia/reperfusion (I/R)-induced kidney injury based on the Keap1-Nrf2/ARE signaling pathway. *Transl Androl Urol* 2022;11(8):1177-1188.
- 64 Zhu XC, He LJ, Gao W, Zhao ZH. Neuroprotective investigation of tanshinone in the cerebral infarction model in the Keap1-Nrf2/ARE pathway. *Cell Cycle* 2023;22(4):390-402.
- 65 Palsamy P, Bidasee KR, Ayaki M, Augusteyn RC, Chan JY, Shinohara T. Methylglyoxal induces endoplasmic reticulum stress and DNA demethylation in the *Keap1* promoter of human lens epithelial cells and age-related cataracts. *Free Radic Biol Med* 2014;72:134-148.